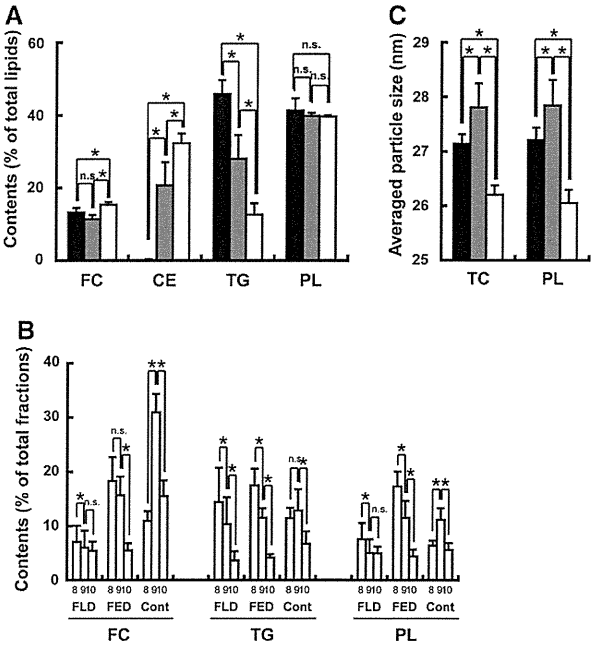

Figure 3. Characterization of lipid profiles in Lp8 of familial lecithin:cholesterol acyltransferase deficiency (FLD) and Fish-eye disease (FED). **A**, Lipid compositions of Fr. 7 to 10 fractions (Lp8) were compared among FLD (closed column), FED (gray column), and normal (open column). *P<0.05. **B**, Lipid concentrations of fractions 8, 9, and 10 were compared in FLD (n=5), FED (n=4), and controls (n=4). *P<0.05. Cholesteryl ester (CE) concentrations in FLD are not shown because levels were undetectable. **C**, Size distribution of lipoproteins in Lp8 (Fr. 7–10) was compared among FLD (closed column), FED (gray column), and normal (open column) based on total cholesterol (TC) and phospholipid (PL) concentrations. *P<0.05. FC indicates free cholesterol; and TG, triglyceride.

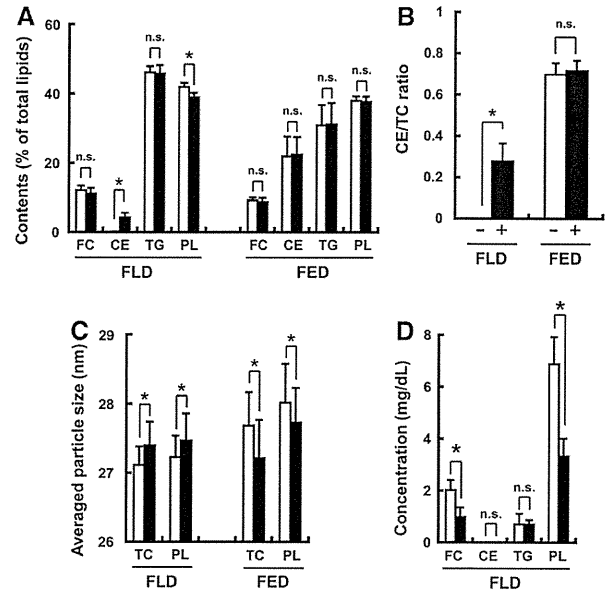

Figure 4. Effects of in vitro familial lecithin:cholesterol acyltransferase (LCAT) supplementation on the lipid profiles of abnormal lipoproteins in LCAT-deficiency syndrome. After analyses described in Figure II in the online-only Data Supplement, lipid composition (**A**), cholesteryl ester (CE)/TC ratio (**B**), averaged particle size based on total cholesterol (TC) and phospholipid (PL) concentrations (**C**), in Lp8, and lipid concentrations in Lp12 to 16 (**D**), were compared between culture media containing recombinant LCAT (rLCAT; closed column) and media without rLCAT (open column). *P<0.05. FC indicates free cholesterol; FED, Fish-eye disease; and TG, triglyceride.

deficiency (Figures 1 and 4B). Lp8 also differed in composition between FLD and FED: in FLD, it contained increased TG and decreased CE in comparison with FED (Figure 3A). Importantly, although the levels varied with the severity of renal damage as did those in Lp1, the buoyance of the peak at Fr. 8 did not vary with severity of renal damage (Figure 2), strongly suggesting that Lp8 directly results from a lack of LCAT and not from metabolic disturbances that occur during proteinuria and progressive renal failure.

In addition to the above-mentioned characteristics for Lp8 in LCAT-deficiency syndrome, HPLC-GFC analyses clarified novel unique lipid properties of Lp8 in FLD in comparison with that in FED; the averaged sizes of Lp8 are smaller in FLD than those in FED (Figure 3C). The lipid compositions of Lp8 in FLD were, in part, ameliorated by rLCAT incubation (Figure 4A). The averaged sizes of the Lp8 increased in FLD, whereas those in FED decreased (Figure 4C). rLCAT increased the CE formation in both LDL and HDL fractions in FLD sera. Thus, these findings indicated that the abnormal compositions were most likely caused primarily by the dysfunction of LCAT in the patients, and that the abnormal characteristics of Lp8 were not because of metabolic disturbances that occur during proteinuria and progressive loss of kidney function.

Previous extensive analyses using electron microscopy have identified 3 abnormal lipoproteins in the LDL fraction of FLD[12]: TG-rich and CE-poor particles of sizes similar to normal LDL (FLD-LDL); FC- and PL-containing particles of sizes distributing from 40 to 60 nm (LpX-like particle)[2]; particles with a diameter of 100 nm (designated as LM-LDL)[17,30] that were later reported to be identical to LpX.[15] LpX is FC- and PL-rich but TG-poor lipid particles (30%, 60%, and 2%, respectively)[22] without apolipoproteins, which range from very low density lipoprotein to large LDL fractions in fast performance liquid chromatography analysis.[31] The abnormal particles have been shown to be decreased by lipid-lowering therapy in a patient with FLD.[21] Lipoproteins in Lp8 were different from LpX in the lipid contents; the fractions were rich in FC and PL and also rich in TG (13.2±1.3%, 41.4±3.3%, and 45.8±3.8%, respectively). The composition analyses suggested that Lp8 corresponds to FLD-LDL, but the calculated sizes of Lp8 were larger than normal LDL using the data obtained by size fractionation with HPLC-GPC in the present study. Thus, the identified Lp8 in LCAT-deficiency syndrome was most likely not identical to LpX in the characteristics.

There is a limitation for the interpretation of the quantitative measurement of LpX in the frozen samples collected in our study because the abnormal lipoproteins were known to be labile to freezing-and-thawing treatment. In this context, fresh sera were collected from patients 2 and 4 and analyzed by agarose gel electrophoresis. The lipid staining of lipoproteins electrophoresed in agarose gel detected the abnormally slowly migrating TG-poor lipoproteins, LpX, at the expectedly migrating position, as well as TG-rich abnormal β-lipoproteins (LDL) in the once-frozen sample, as well as the fresh sample

in patient 4, although the staining intensity tended to decrease in comparison with the fresh counterpart. However, LpX was not detected in either sample with or without freeze-and-thaw treatment from patient 2. Thus, LpX was indeed labile to freeze/thawing, and the frozen samples were not adequate for the quantitative measurement. However, the presence was still able to be evaluated after once-freezing treatment. On the basis of background data, HPLC-GFC analysis showed that lipid contents in Lp8 were not largely affected by once-freezing treatment in both patients 2 and 4: in contrast, the contents of TG and PL were slightly decreased in lipoproteins with peak of Fr. 5 (data not shown). Additional studies using fresh samples of patients with distinct mutations and manifestations are needed to interpret the significance of novel lipoproteins in comparison with LpX for the development of renal insufficiency in LCAT0deficiency syndrome quantitatively.

In FLD but not in FED, Lp12 to 16 were heterogeneous in size and rich in PL. rLCAT decreased PL in these fractions specifically (Figure 5D; Figure II in the online-only Data Supplement). This may suggest that the heterogeneous-sized PL-rich particles in Fr. 12 to 16 converge to normal-sized HDL (Fr. 16–18) on incubation with rLCAT, with concomitant esterification of FC.

In conclusion, 4 lipoprotein fractions specific to LCAT-deficiency syndromes were identified by the HPLC-GFC analysis of samples from genetically diagnosed patients with different mutations and manifestations. The composition of 2 of these was unique to only FLD; these were not likely compatible with the previously reported LpX. These abnormal lipoproteins may be causal to the renal pathology in FLD, the main cause of increased morbidity and mortality in this condition. The regular evaluation of these specific lipid fractions during LCAT enzyme replacement therapy in patients with LCAT deficiency may provide guidance for success of the intervention. The value of these lipid fractions for risk of future renal disease needs to be addressed in prospective follow-up studies in patients with FLD with various mutations in the *LCAT* gene before the onset of proteinuria.

Sources of Funding

This study was supported, in part, by Health and Labour Sciences Research grants for translational research and for research on rare and intractable diseases, Japan (Hideaki Bujo). A.G. Holleboom is supported by a Veni grant (project number 91613031) from the Netherlands Organization of Research NWO.

Disclosures

None.

References

1. Glomset JA, Assmann G, Gjone E, Norum KR. Lecithin cholesterol acyltransferase deficiency and fish eye disease. In: Scriver CR, Beaudet AL, Sly WS, Valle D, Stanbury JB, Wyngaarden JB, Fredrickson DS, eds. *The Metabolic and Molecular Bases of Inherited Disease*, 7th ed. New York, NY: McGraw-Hill Inc; 1995:1933–1951.
2. Santamarina-Fojo S, Hoeg JM, Assman G, Brewer HB Jr. Lecithin cholesterol acyltransferase deficiency and fish eye disease. In: Scriver CR, Beaudet AL, Sly WS, Valle D, Childs B, Kinzler KW, Vogelstein B, eds. *The Metabolic and Molecular Bases of Inherited Disease*, 8th ed. New York, NY: McGraw-Hill Inc;2001:2817–2833.
3. Human Gene Mutation Database. 2013. *Human Gene Mutation Database*. http://www.hgmd.org.
4. *The Online Metabolic and Molecular Bases of Inherited Diseases (OMMBID), part 12: LIPIDS*, http://www.ommbid.com/OMMBID/the_online_metabolic_and_molecular_bases_of_inherited_disease/b/abstract/part12/ch118.
5. Séguret-Macé S, Latta-Mahieu M, Castro G, Luc G, Fruchart JC, Rubin E, Denèfle P, Duverger N. Potential gene therapy for lecithin-cholesterol acyltransferase (LCAT)-deficient and hypoalphalipoproteinemic patients with adenovirus-mediated transfer of human LCAT gene. *Circulation*. 1996;94:2177–2184.
6. Rousset X, Vaisman B, Auerbach B, Krause BR, Homan R, Stonik J, Csako G, Shamburek R, Remaley AT. Effect of recombinant human lecithin cholesterol acyltransferase infusion on lipoprotein metabolism in mice. *J Pharmacol Exp Ther*. 2010;335:140–148.
7. Kuroda M, Bujo H, Aso M, Saito Y. Adipocytes as a vehicle for ex vivo gene therapy: novel replacement therapy for diabetes and other metabolic diseases. *J Diabetes Invest*. 2011;2:333–340.
8. Chen Z, Chu D, Castro-Perez JM, et al. AAV8-mediated long-term expression of human LCAT significantly improves lipid profiles in hCETP;Ldlr(+/-) mice. *J Cardiovasc Transl Res*. 2011;4:801–810.
9. Kuroda M, Aoyagi Y, Asada S, Bujo H, Tanaka S, Konno S, Tanio M, Ishii I, Machida K, Matsumoto F, Satoh K, Aso M, Saito Y. Ceiling culture-derived proliferative adipocytes are a possible delivery vehicle for enzyme replacement therapy in lecithin: cholesterol acyltransferase deficiency. *Open Gene Ther J*. 2011;4:1–10.
10. Asada S, Kuroda M, Aoyagi Y, Bujo H, Tanaka S, Konno S, Tanio M, Ishii I, Aso M, Saito Y. Disturbed apolipoprotein A-I-containing lipoproteins in fish-eye disease are improved by the lecithin:cholesterol acyltransferase produced by gene-transduced adipocytes *in vitro*. *Mol Genet Metab*. 2011;102:229–231.
11. Glomset JA, Nichols AV, Norum KR, King W, Forte T. Plasma lipoproteins in familial lecithin: cholesterol acyltransferase deficiency. Further studies of very low and low density lipoprotein abnormalities. *J Clin Invest*. 1973;52:1078–1092.
12. Forte T, Nichols A, Glomset J, Norum K. The ultrastructure of plasma lipoproteins in lecithin:cholesterol acyltransferase deficiency. *Scand J Clin Lab Invest Suppl*. 1974;137:121–132.
13. Glomset JA, Norum KR, King W. Plasma lipoproteins in familial lecithin: cholesterol acyltransferase deficiency: lipid composition and reactivity *in vitro*. *J Clin Invest*. 1970;49:1827–1837.
14. Norum KR, Glomset JA, Nichols AV, Forte T. Plasma lipoproteins in familial lecithin: cholesterol acyltransferase deficiency: physical and chemical studies of low and high density lipoproteins. *J Clin Invest*. 1971;50:1131–1140.
15. Guérin M, Dolphin PJ, Chapman MJ. Familial lecithin:cholesterol acyltransferase deficiency: further resolution of lipoprotein particle heterogeneity in the low density interval. *Atherosclerosis*. 1993;104:195–212.
16. Gjone E. Familial lecithin:cholesterol acyltransferase deficiency—a clinical survey. *Scand J Clin Lab Invest Suppl*. 1974;137:73–82.
17. Gjone E, Blomhoff JP, Skarbovik AJ. Possible association between an abnormal low density lipoprotein and nephropathy in lecithin: cholesterol acyltransferase deficiency. *Clin Chim Acta*. 1974;54:11–18.
18. Guerin M, Dachet C, Goulinet S, Chevet D, Dolphin PJ, Chapman MJ, Rouis M. Familial lecithin:cholesterol acyltransferase deficiency: molecular analysis of a compound heterozygote: LCAT (Arg147 -> Trp) and LCAT (Tyr171 -> Stop). *Atherosclerosis*. 1997;131:85–95.
19. Lambert G, Sakai N, Vaisman BL, et al. Analysis of glomerulosclerosis and atherosclerosis in lecithin cholesterol acyltransferase-deficient mice. *J Biol Chem*. 2001;276:15090–15098.
20. Zhu X, Herzenberg AM, Eskandarian M, Maguire GF, Scholey JW, Connelly PW, Ng DS. A novel *in vivo* lecithin-cholesterol acyltransferase (LCAT)-deficient mouse expressing predominantly LpX is associated with spontaneous glomerulopathy. *Am J Pathol*. 2004;165:1269–1278.
21. Yee MS, Pavitt DV, Richmond W, Cook HT, McLean AG, Valabhji J, Elkeles RS. Changes in lipoprotein profile and urinary albumin excretion in familial LCAT deficiency with lipid lowering therapy. *Atherosclerosis*. 2009;205:528–532.
22. Lynn EG, Choy PC, Magil A, O K. Uptake and metabolism of lipoprotein-X in mesangial cells. *Mol Cell Biochem*. 1997;175:187–194.
23. Holleboom AG, Kuivenhoven JA, van Olden CC, Peter J, Schimmel AW, Levels JH, Valentijn RM, Vos P, Defesche JC, Kastelein JJ, Hovingh GK, Stroes ES, Hollak CE. Proteinuria in early childhood due to familial LCAT deficiency caused by loss of a disulfide bond in lecithin:cholesterol acyl transferase. *Atherosclerosis*. 2011;216:161–165.
24. Naito S, Kamata M, Furuya M, Hayashi M, Kuroda M, Bujo H, Kamata K. Amelioration of circulating lipoprotein profile and proteinuria in a patient

with LCAT deficiency due to a novel mutation (Cys74Tyr) in the lid region of LCAT under a fat-restricted diet and ARB treatment. *Atherosclerosis*. 2013;228:193–197.
25. Wang XL, Osuga J, Tazoe F, Okada K, Nagashima S, Takahashi M, Ohshiro T, Bayasgalan T, Yagyu H, Okada K, Ishibashi S. Molecular analysis of a novel LCAT mutation (Gly179 → Arg) found in a patient with complete LCAT deficiency. *J Atheroscler Thromb*. 2011;18:713–719.
26. Asztalos BF, Schaefer EJ, Horvath KV, Yamashita S, Miller M, Franceschini G, Calabresi L. Role of LCAT in HDL remodeling: investigation of LCAT deficiency states. *J Lipid Res*. 2007;48:592–599.
27. Holleboom AG, Kuivenhoven JA, Peelman F, Schimmel AW, Peter J, Defesche JC, Kastelein JJ, Hovingh GK, Stroes ES, Motazacker MM. High prevalence of mutations in LCAT in patients with low HDL cholesterol levels in The Netherlands: identification and characterization of eight novel mutations. *Hum Mutat*. 2011;32:1290–1298.
28. Hovingh GK, Hutten BA, Holleboom AG, Petersen W, Rol P, Stalenhoef A, Zwinderman AH, de Groot E, Kastelein JJ, Kuivenhoven JA. Compromised LCAT function is associated with increased atherosclerosis. *Circulation*. 2005;112:879–884.
29. Friedewald WT, Levy RI, Fredrickson DS. Estimation of the concentration of low-density lipoprotein cholesterol in plasma, without use of the preparative ultracentrifuge. *Clin Chem*. 1972;18:499–502.
30. Glomset JA, Norum KR, Nichols AV, King WC, Mitchell CD, Applegate KR, Gong EL, Gjone E. Plasma lipoproteins in familial lecithin: cholesterol acyltransferase deficiency: effects of dietary manipulation. *Scand J Clin Lab Invest Suppl*. 1975;142:3–30.
31. Nishiwaki M, Ikewaki K, Bader G, Nazih H, Hannuksela M, Remaley AT, Shamburek RD, Brewer HB Jr. Human lecithin:cholesterol acyltransferase deficiency: *in vivo* kinetics of low-density lipoprotein and lipoprotein-X. *Arterioscler Thromb Vasc Biol*. 2006;26:1370–1375.

Significance

Lecithin:cholesterol acyltransferase-deficiency syndromes are classified into 2 forms: familial lecithin:cholesterol acyltransferase deficiency and fish-eye disease. Patients with familial lecithin:cholesterol acyltransferase deficiency develop renal failure, whereas fish-eye disease patients do not. This study was performed to identify abnormal lipoproteins associated with the renal damage of patients with different mutations and manifestations. Size fractionation with gel filtration of patients' sera and in vitro incubation experiments with recombinant lecithin:cholesterol acyltransferase showed abnormal lipoproteins associated with the renal damage. Thus, our novel analytic approach identified large low-density lipoprotein and high-density lipoprotein with a composition specific to familial lecithin:cholesterol acyltransferase deficiency but not to fish-eye disease. The identification of abnormal lipoproteins may shed light on the clarification of renal pathology and the development of treatment for the patients with familial lecithin:cholesterol acyltransferase deficiency.

Materials and methods

Identification of FLD and FED patients

Patients were referred because of a clinical suspicion of LCAT deficiency due to the presence of corneal opacification and HDL deficiency, with or without proteinuria and/or renal insufficiency (Table 1). Lipid profiles of the patients are also given in Table 2. In our clinics, the definitive molecular diagnoses were established for all patients. The renal biopsy analyses were performed to make a diagnosis for renal damage in some patients. Patient(Pt)s 1 and 3 are Morroccan sister[24]. Other patients are unrelated. Pt.2 was treated with a fat-restricted diet (1570 kcal; fat 10 g and protein 45 g) during admission, with the prescription of losartan 50 mg/day for 8 months. Younger sister of Pt. 2 also shows corneal opacification. Informed consent from her was not obtained for genetic analysis and current study. Proteinuria for FLD patients were 6g/24h (Pt. 1), 2 g/24h (Pt. 2), 0.45 g/l (Pt. 3), 0.23g/24h (Pt. 4), and 0.5 g/l (Pt. 5).

Analysis of patient samples

This study was approved by the Ethics Committees of Chiba University School of Medicine and Academic Medical Center, University of Amsterdam, and informed consent was obtained from the participants including unaffected normolipidemic controls. Blood samples were obtained from participants, and serum was prepared and stored at -80 °C until use. LCAT activity (α-activity) was measured using artificial proteoliposomes as substrate[1]. Serum lipoproteins were fractionated by high-performance liquid chromatography with gel filtration column (HPLC-GFC)[2,3] and analyzed simultaneously by online enzymatic method to quantify total cholesterol (TC), free cholesterol (FC), triglyceride (TG), and phospholipid (PL) (Skylight Biotech, Akita, Japan). The resulting raw chromatograms (elution time versus lipid concentration) were further processed by computer program with the modified Gaussian curve fitting for resolving the overlapping peaks by mathematical treatment. Finally, the system subdivided the lipoprotein particles of normal subjects by size into the following 20 subclasses: chylomicron (CM, >80 nm, fractions 1-2), very low density lipoprotein (VLDL, 30-80 nm, fractions 3-7), low density lipoprotein (LDL, 16-30 nm, fractions 8-13), and high density lipoprotein (HDL, 8-16 nm, fractions 14-20). In this fractionation analysis, standard particle diameters have been reported to be >90, 75, 64, 53.6, 44.5, 36.8, 31.3, 28.6, 25.5, 23.0, 20.7, 18.6, 16.7, 15.0, 13.5, 12.1, 10.9, 9.8, 8.8, 7.6 nm for fraction 1 through 20, respectively[2]. Average sizes of lipoprotein

classes were calculated based on the particle diameter as follows: (sum of particle diameter x lipid concentration in each fraction)/(sum of lipid concentration of the fractions of interest). Ultracentrifugation fractionation followed by determination of lipid contents was performed in Pt. 1, 2 and 5 (Table I in data supplement). For some FLD sera, representative fractions were collected, concentrated by Vivaspin (MWCO=3,000, Sartorius, Weender Landstr., Germany) and subjected to determine apolipoprotein concentrations by Milliplex MAP Human Apolipoprotein Panel kit (Millipore, Billerica, MA) using BioPlex apparatus (BioRad, Hercules, CA).

Preparation of recombinant LCAT and *in vitro* incubation with patient's serum

Human *LCAT* gene was transduced into human preadipocytes by retroviral vector as described previously[1]. The resulting cells were seeded into T225 flask and grown to confluency in MesenPRO medium (Life Technologies, Carlsbad, CA). The medium was changed to 30 ml of OPTI MEM I (Life Technologies) and the cells were further incubated for seven days to collect culture supernatant. The culture supernatant was concentrated to one-fiftieth of the original volume by Amicon Ultra (MWCO=50 kDa, Millipore)[4]. LCAT concentration was titrated by immunoblotting using commercially available human rLCAT (Roar Biomedical, Inc., Calverton, NY) as standard. After mixing with rLCAT-containing culture supernatant at the ratio of 29:71 (v/v), each patient's serum was incubated at 37 °C for 24 hr (final concentration of rLCAT was 6 μg/ml), and subjected to lipoprotein analysis. Culture supernatant of human preadipocytes without gene transduction was used as control.

Statistical analysis

Data are presented as means ± S.D. Comparisons were assessed for significant differences by paired Student's *t*-test, or by ANOVA followed by Tukey test, where appropriate. SPSS software was used for statistical analyses. In all cases, P values of less than 0.05 were considered significant.

REFERENCES:

1. Kuroda M, Aoyagi Y, Asada S, Bujo H, Tanaka S, Konno S, Tanio M, Ishii I, Machida K, Matsumoto F, Satoh K, Aso M, Saito Y. Ceiling culture-derived

proliferative adipocytes are a possible delivery vehicle for enzyme replacement therapy in lecithin: cholesterol acyltransferase deficiency. *The Open Gene Ther J* 2011;4:1-10

2. Okazaki M, Usui S, Ishigami M, Sakai N, Nakamura T, Matsuzawa Y, Yamashita S. Identification of unique lipoprotein subclasses for visceral obesity by component analysis of cholesterol profile in high-performance liquid chromatography. *Arterioscler Thromb Vasc Biol* 2005;25:578-584
3. Usui S, Hara Y, Hosaki S, Okazaki M. A new on-line dual enzymatic method for simultaneous quantification of cholesterol and triglycerides in lipoproteins by HPLC. *J Lipid Res* 2002;43:805-814
4. Asada A, Kuroda M, Aoyagi Y, Bujo H, Tanaka S, Konno S, Tanio M, Ishii I, Aso M, Saito Y. Disturbed apolipoprotein A-I-containing lipoproteins in fish-eye disease are improved by the lecithin:cholesterol acyltransferase produced by gene-transduced adipocytes *in vitro*. *Mol Genet Metab* 2010;102:229-231

Supplement Table I

		Pt. 1	Pt. 2	Pt. 5
HDL				
	Total cholesterol (mg/dl)	18.6	12.0	10.8
	Triglyceride (mg/dl)	3.6	3.0	4.2
	Phospholipid (mg/dl)	65.4	44.4	42.0
LDL				
	Total cholesterol (mg/dl)	62.4	99.0	39.6
	Triglyceride (mg/dl)	77.4	151.2	61.8
	Phospholipid (mg/dl)	106.2	157.8	73.2
VLDL				
	Total cholesterol (mg/dl)	62.0	51.0	9.6
	Triglyceride (mg/dl)	190.0	157.8	36.0
	Phospholipid (mg/dl)	103.4	81.8	21.8

Supplement Table I. Ultracentrifugation analysis of lipoprotein in FLD patients.
Patients' sera were subjected to ultracentrifugation fractionation, followed by determination of lipid concentration.

Supplement Figure I

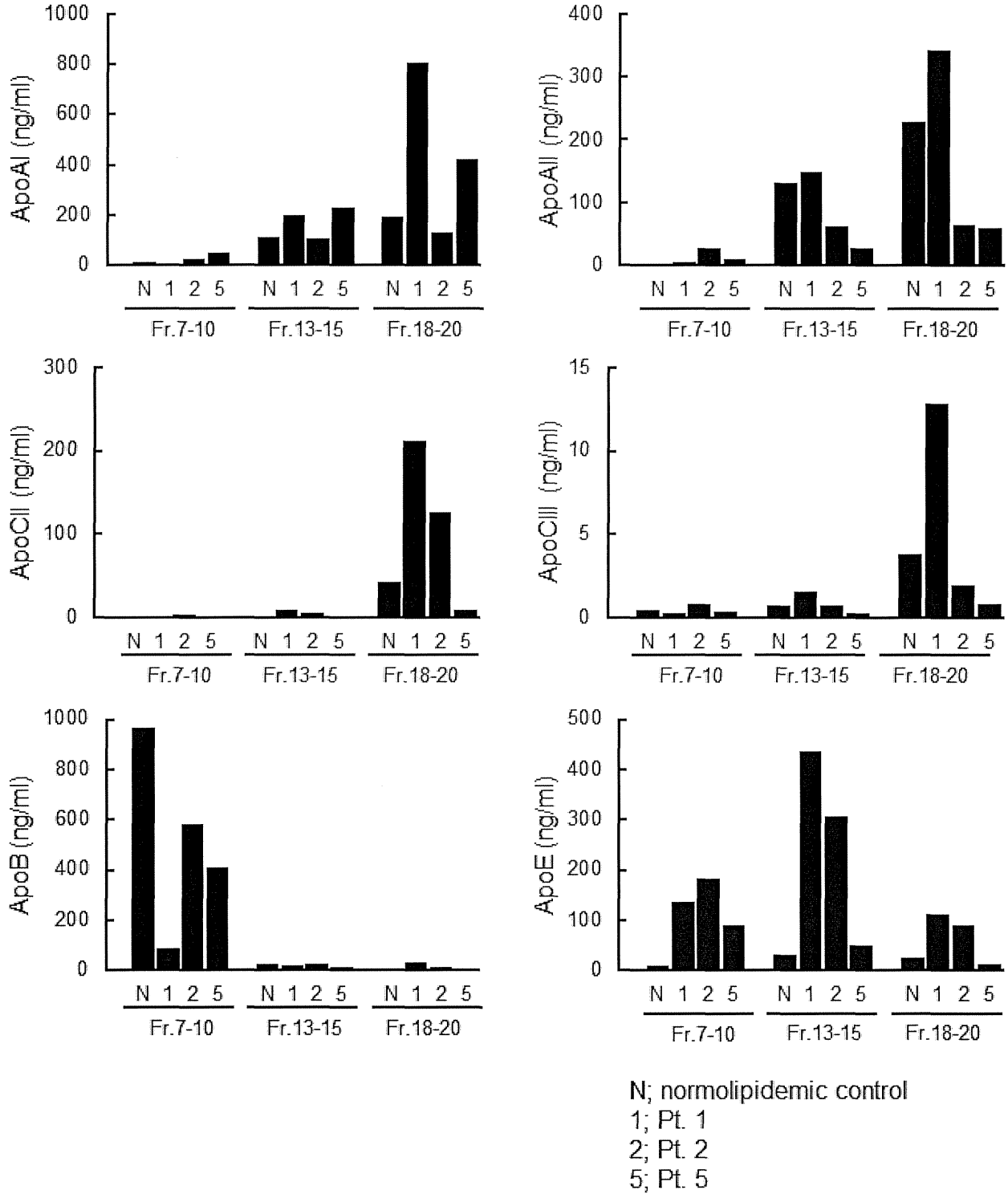

Supplement Figure I. Apolipoprotein contents in lipoproteins in FLD patients.
Lipoprotein subfractions were collected and concentrated (MWCO=3,000). Apolipoprotein concentrations in the concentrated samples were determined by ELISA. N; normolipidemic control, 1; Pt. 1, 2; Pt. 2, 5; Pt. 5.

Supplement Figure II

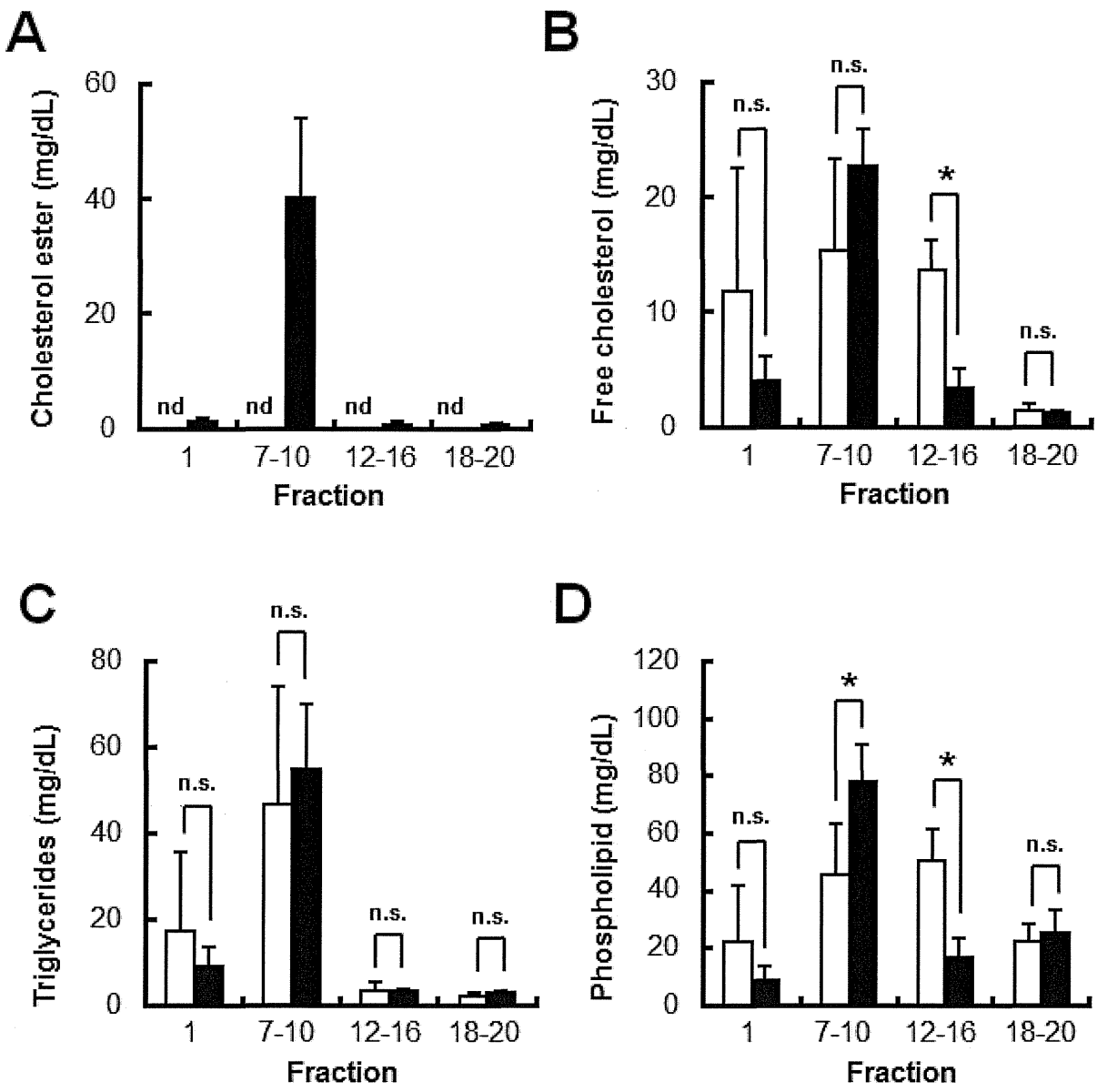

Supplement Figure II. Comparison of lipid concentrations of lipoproteins between FLD and FED.

According to the distribution of lipoproteins shown in Figure 1, CE (panel A), FC (panel B), TG (panel C), and PL (panel D) concentrations in Fr. 1, Fr. 7-10, Fr. 12-16 and Fr. 18-20 were compared between FLD patients (open column, n=5) and FED patients (closed column, n=4). nd, not detected, *$p<0.05$.

Supplement Figure III

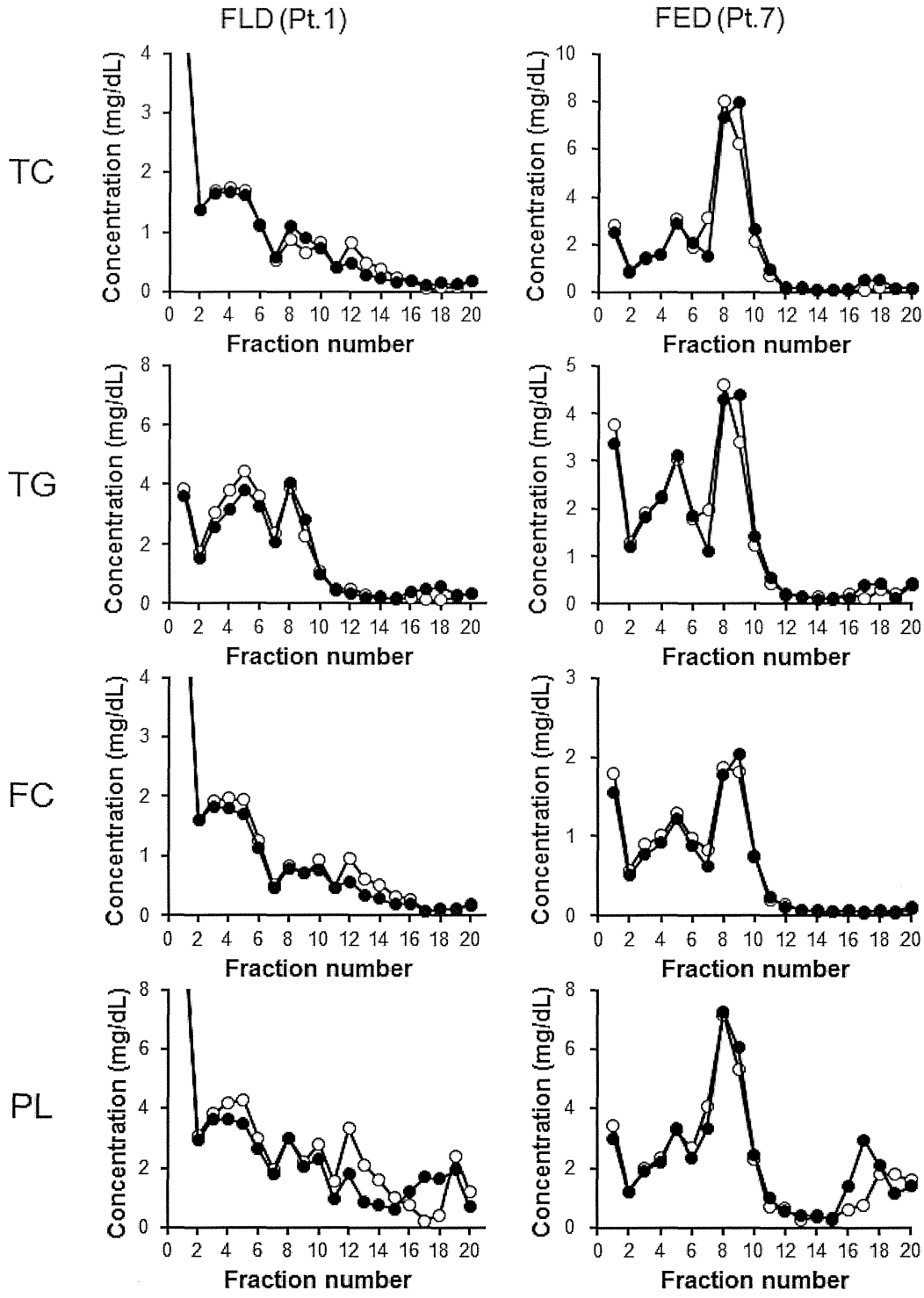

Supplement Figure III. Response to rLCAT *in vitro*

After incubation with culture supernatant of human *LCAT* gene-transduced preadipocytes (closed circle) and un-transduced control (open circle), GFC analyses with simultaneous determination of TC, TG, FC, and PL concentrations were performed. Representative results of FLD (Pt. 1) and FED (Pt. 7) sera were shown.

Supplement Figure IV

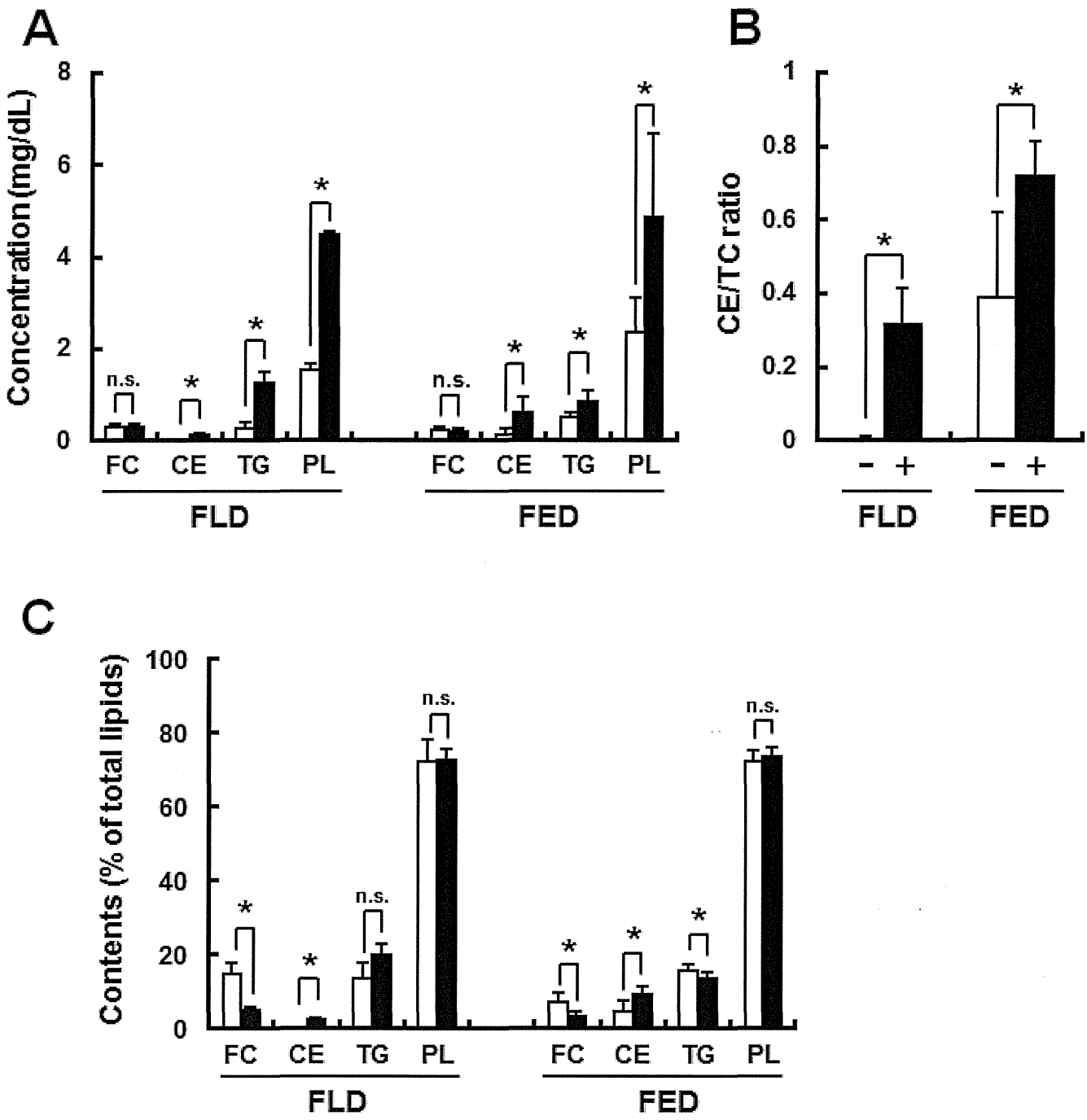

Supplement Figure IV. *In vitro* rLCAT incubation ameliorated HDL composition in FLD and FED.

After *in vitro* rLCAT incubation and subsequent GFC analyses of lipoproteins shown in Fig. S2, changes of core HDL fractions (Fr. 16-18) were analyzed in FLD (n=4) and FED (n=4) sera (A-C). Lipid concentrations (A), CE/TC ratio (B), and lipid composition (C) were compared between rLCAT containing culture media (closed bar) and the culture media without rLCAT (open bar). *p<0.05.

Liver-Specific Deletion of 3-Hydroxy-3-Methylglutaryl Coenzyme A Reductase Causes Hepatic Steatosis and Death

Shuichi Nagashima, Hiroaki Yagyu, Ken Ohashi, Fumiko Tazoe, Manabu Takahashi, Taichi Ohshiro, Tumenbayar Bayasgalan, Kenta Okada, Motohiro Sekiya, Jun-ichi Osuga, Shun Ishibashi

Objective—3-hydroxy-3-methylglutaryl coenzyme A reductase (HMGCR) catalyzes the rate-limiting step in cholesterol biosynthesis and has proven to be an effective target of lipid-lowering drugs, statins. The aim of this study was to understand the role of hepatic HMGCR in vivo.

Methods and Results—To disrupt the HMGCR gene in liver, we generated mice homozygous for a floxed HMGCR allele and heterozygous for a transgene encoding Cre recombinase under the control of the albumin promoter (liver-specific HMGCR knockout mice). Ninety-six percent of male and 71% of female mice died by 6 weeks of age, probably as a result of liver failure or hypoglycemia. At 5 weeks of age, liver-specific HMGCR knockout mice showed severe hepatic steatosis with apoptotic cells, hypercholesterolemia, and hypoglycemia. The hepatic steatosis and death were completely reversed by providing the animals with mevalonate, indicating its essential role in normal liver function. There was a modest decrease in hepatic cholesterol synthesis in liver-specific HMGCR knockout mice. Instead, they showed a robust increase in the fatty acid synthesis, independent of sterol regulatory element binding protein-1c.

Conclusion—Hepatocyte HMGCR is essential for the survival of mice, and its abrogation elicits hepatic steatosis with jaundice and hypoglycemia. (***Arterioscler Thromb Vasc Biol.* 2012;32:1824-1831.**)

Key Words: cholesterol ■ liver ■ 3-hydroxy-3-methylglutaryl coenzyme A ■ fatty acids ■ knockout mouse

The mevalonate pathway produces isoprenoids that are essential for the diverse cellular functions ranging from cholesterol synthesis to growth control. The enzyme 3-hydroxy-3-methylglutaryl-coenzyme A reductase (HMGCR) (EC 1.1.1.34), which catalyzes the conversion of HMG-coenzyme A to mevalonate, is the rate-limiting enzyme in the mevalonate pathway.[1] Mammalian HMGCR is an integral high-mannose glycoprotein of the endoplasmic reticulum (ER).[2] Structurally, it is divided into 2 major domains: a C-terminal cytosol-facing domain that tetramerizes to form the active site and an N-terminal hydrophobic region that spans the ER membrane 8× and bears a single N-glycan. This membrane region is dispensable for the enzymatic activity but necessary for the metabolically controlled stability of the enzyme and sufficient to cause sterol-accelerated degradation of heterologous proteins. Within this region, transmembrane spans 2 through 6 bear significant sequence homology to the corresponding transmembrane spans of sterol regulatory element binding protein (SREBP) cleavage-activating protein (SCAP).[3]

To ensure a steady supply of mevalonate, the nonsterol and sterol end products of the mevalonate metabolism exert feedback regulatory effects on the activity of this enzyme through multivalent mechanisms, including inhibition of the transcription of its RNA, blocking of translation, and acceleration of the protein's degradation by a mechanism called ER-associated degradation, thereby regulating the amount of protein over a several hundred-fold range. ER-associated degradation of HMGCR requires the binding of Insig-1 to the sterol-sensing domain.[4] Despite the critical role of HMGCR in cholesterol biosynthesis, little is known about its relevance to diseases. Only recently, HMGCR has been identified as a determinant of plasma cholesterol levels.[5]

Inhibitors of HMGCR, statins, are potent cholesterol-lowering agents that have been widely used to prevent the occurrence of coronary heart disease and other atherosclerotic diseases.[6] The atheroprotective properties of statins are primarily because of the potent low-density lipoprotein (LDL)-cholesterol–lowering effect.[7] Statins have also been reported to exert cholesterol-independent, or so-called pleiotropic, effects that involve improving endothelial function and decreasing oxidative stress and vascular inflammation.[8] The benefits of statins extend beyond cardiovascular diseases and include a reduction in the risk of dementia, Alzheimer disease, ischemic stroke, osteoporosis, tumor growth, and viral infection. Most of these pleiotropic effects are mediated by an ability to block the synthesis of nonsterol isoprenoid intermediates. Statins have toxic effects in only a limited number of patients and are generally considered safe.

Received on: May 2, 2011; final version accepted on: April 30, 2012.

From the Division of Endocrinology and Metabolism, Department of Medicine, Jichi Medical University, Shimotsuke, Tochigi, Japan (S.N., H.Y., F.T., M.T., T.O., T.B., K. Okada, J.O., S.I.); and Department of Metabolic Diseases, Graduate School of Medicine, University of Tokyo, Tokyo, Japan (K. Ohashi, M.S.).

The online-only Data Supplement is available with this article at http://atvb.ahajournals.org/lookup/suppl/doi:10.1161/ATVBAHA.111.240754/-/DC1.

Correspondence to Shun Ishibashi, MD, PhD, Division of Endocrinology and Metabolism, Department of Medicine, Jichi Medical University, 3311-1 Yakushiji, Shimotsuke, Tochigi 329-0498, Japan. E-mail ishibash@jichi.ac.jp

Arterioscler Thromb Vasc Biol **is available at http://atvb.ahajournals.org** **DOI: 10.1161/ATVBAHA.111.240754**

To establish an animal model for investigating the mechanisms behind the effects, including toxicity of statins, we have generated HMGCR knockout (KO) mice lacking the enzyme throughout their bodies.[9] These mice die in a relatively early stage of embryonic development (ie, before E8.5). Because mice lacking squalene synthase, the first committed enzyme in the sterol pathway, die in the embryonic stage with apparent anomalies of the development of the central nervous system,[10] we took advantage of the tissue-specific gene targeting using the Cre-loxP system to generate mice lacking HMGCR in a liver-specific manner.

Materials and Methods

Liver-specific HMGCRKO (L-HMGCRKO) mice were generated by cross-breeding heterozygous floxed HMGCR (referred to as $HMGCR^{+/f}$; f denotes floxed) mice with transgenic mice expressing Cre recombinase under the control of albumin gene promoter (Alb-Cre).[11,12] All animal experiments were performed with the approval of the Institutional Animal Care and Research Advisory Committee at Jichi Medical University. For detailed protocols for the generation of L-HMGCRKO mice and other experimental procedures, please refer to the online-only Data Supplement.

Results

Because there were no differences in growth curves or metabolic parameters, such as plasma lipid and glucose levels, among the $HMGCR^{+/+}$ (wild-type), $HMGCR^{+/+}$ Alb-Cre (CRE), and $HMGCR^{f/f}$ (fHMGCR) mice, we used fHMGCR mice as a control. To determine whether the expression of the HMGCR gene was abrogated in the liver, we performed a Southern blot (Figure 1A), Northern blot (Figure 1B), and real-time polymerase chain reaction (Figure 1C). The Southern blot analysis shows that only the 6.3-kb wild-type allele and 7.7-kb floxed allele were observed in the DNA from liver in wild-type and fHMGCR mice, respectively. In L-HMGCRKO mice at 3 weeks, the liver contained predominantly the 12.0-kb KO allele (70% based on PhosphorImager analysis [BAS 200, Fujifilm, Tokyo, Japan]) and some residual floxed allele (30%). The mRNA expression of HMGCR in the liver of L-HMGCRKO mice was decreased to 30% of the fHMGCR mice at 3 weeks of age and to <10% at 4 and 5 weeks upon Northern blot analysis. The time-dependent abrogation of the mRNA expression of HMGCR was also confirmed by real-time polymerase chain reaction. Based on this method, the mRNA levels were decreased to only 2% of the fHMGCR mice at 4 and 5 weeks, although there were no significant differences in other organs (Figure IIA in the online-only Data Supplement). Immunoblot analysis showed that the amount of HMGCR protein in the liver of L-HMGCRKO mice was 15% of that in fHMGCR mice (Figure 1D). Despite the profound reduction in HMGCR at both the mRNA and protein levels, the HMGCR activity in the liver of L-HMGCRKO mice was decreased by only 44% compared with that in fHMGCR mice (Figure 1E). To determine whether HMGCR is specifically abrogated in the liver parenchymal cells of L-HMGCRKO mice, we separated parenchymal and nonparenchymal cells from the liver at 3 weeks of age by density-gradient centrifugation after liver perfusion with collagenase. The mRNA expression of HMGCR in the parenchymal cells of L-HMGCRKO mice was decreased by 70.6% compared with that in fHMGCR mice, whereas the mRNA expression of HMGCR in the nonparenchymal cells was not different between the fHMGCR and L-HMGCRKO mice at 3 weeks of age (Figure IIC in the

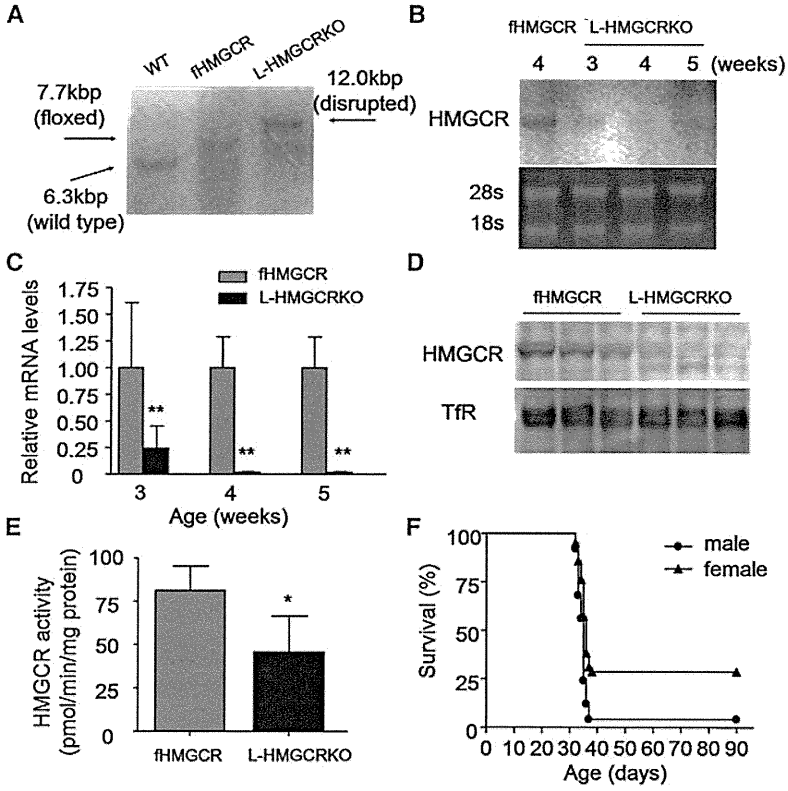

Figure 1. Conditional deletion of the 3-hydroxy-3-methylglutaryl-coenzyme A reductase (HMGCR) gene in mice and their survival. **A**, Southern blot analysis of *BamHI*-digested DNA from the livers of wild-type (WT) floxed HMGCR (fHMGCR) and liver-specific HMGCR knockout (L-HMGCRKO) mice at 3 weeks of age as described in the online-only Data Supplement. **B**, Northern blot analysis of hepatic RNA from the livers of fHMGCR and L-HMGCRKO mice at 3, 4, and 5 weeks of age. Aliquots (20 μg) of total RNA from liver were subjected to electrophoresis and blot hybridization with ^{32}P-labeled cDNA probes for mouse HMGCR as described in the online-only Data Supplement. **C**, Quantitative real-time polymerase chain reaction of HMGCR mRNA levels from the livers of mice indicated in **B** (n=5 in each group). **D**, Immunoblot analysis of HMGCR protein from the livers of control and L-HMGCRKO mice at 4 weeks of age (n=3 in each group). Aliquots (50 μg) of liver membrane fractions were subjected to SDS-PAGE and immunoblot analysis. The membrane protein transferrin receptor was used as a loading control. **E**, HMGCR activity in the liver microsomal fractions of fHMGCR and L-HMGCRKO mice at 4 weeks of age (n=5 in each group). **F**, The survival curves were generated by the Kaplan-Meier method, and differences among the survival rates were compared using the χ^2 method. Male (n=25) and female (n=42) L-HMGCRKO mice were followed for >100 days. Each value represents mean±SD. Significant differences compared with control mice: **P*<0.05 and ***P*<0.001.

Table. Liver Weight and Plasma Parameters of Control and L-HMGCRKO Mice

Age (wks)	3		4		5	
Genotype	fHMGCR (n=5)	L-HMGCRKO (n=5)	fHMGCR (n=9)	L-HMGCRKO (n=7)	fHMGCR (n=6)	L-HMGCRKO (n=5)
Body weight (g)	10.6±1.3	11.7±1.5	17.2±1.3	15.5±0.8*	21.7±2.0	13.5±0.8***
Liver weight (g)	0.47±0.11	0.51±0.11	0.78±0.14	0.92±0.13	1.08±0.11	1.17±0.28
Liver/body weight (%)	4.4±0.4	4.2±0.4	4.4±0.4	6.1±0.8*	5.0±0.12	8.7±2.1**
Total cholesterol (mg/dL)	63.6±9.1	47.1±1.0**	66.5±11.1	46.7±13.2**	64.6±6.8	282.6±72.6***
Free cholesterol (mg/dL)	26.2±4.0	20.1±0.5*	33.3±5.5	24.6±13.5	33.1±2.7	263.0±72.6***
Cholesterol ester (mg/dL)	37.4±5.5	27.0±1.4*	33.1±5.7	22.1±4.6*	31.5±4.9	19.6±10.3
Triglyceride (mg/dL)	62.5±13.3	51.1±9.9	78.5±25.4	24.9±6.9***	92.5±31.1	27.7±9.4**
Free fatty acids (mmol/L)	0.34±0.10	0.40±0.06	0.63±0.20	0.51±0.19	0.55±0.09	1.70±0.92*
Phospholipids (mg/dL)	132.2±20.2	106±2.7*	143.5±22.8	117.3±31.7	150.9±12.3	601.1±133.5**
Aspartate aminotransferase (IU/L)	76.1±10.2	95.7±45.5	92.7±39.3	343.1±602.8	55.9±18.6	1178.5±182.1***
Alanine transaminase (IU/L)	35.1±12.1	61.9±46.7	20.7±17.5	54.2±101.7	13.1±4.6	878.8±357.6**
Total bilirubin (mg/dL)	0.31±0.09	0.31±0.09	0.30±0.08	0.36±0.29	0.33±0.19	3.25±1.69*
Blood glucose (mg/dL)	110.6±16.7	123.0±15.5	115.9±13.7	99.6±16.7	135.7±9.4	48.3±23.3*

Blood samples were taken from male mice fed a normal chow diet ad libitum before the study. Each value represents the mean±SD. Significant differences compared with control mice: *P<0.05, **P<0.01, and ***P<0.001. HMGCR indicates 3-hydroxy-3-methylglutaryl-coenzyme A reductase; L-HMGCRKO, liver-specific HMGCR knockout mice; fHMGCR, floxed HMGCR.

online-only Data Supplement). HMGCR activity in the parenchymal cells of L-HMGCRKO mice was decreased by only 47% compared with that in fHMGCR mice (Figure IID in the online-only Data Supplement). The relative decreases in the mRNA and activity of HMGCR in the parencymal cells were similar to those observed in the whole liver of L-HMGCRKO mice (Figure 1C and E), supporting that HMGCR gene was specifically abrogated in the parenchymal cells of the liver and that there was no compensatory upregulation of HMGCR in the nonparenchymal cells of the L-HMGCRKO mice.

L-HMGCRKO mice were born at a rate in accordance with the rule of Mendelian inheritance. However, 96% of males died with a median survival time of 35 days, whereas 71% of females died with a median survival time of 36 days (Figure 1F), and the rest of them survived until 12 months of age. Therefore, the survival rate of females was significantly higher than males (P=0.025). The mRNA expression levels of HMGCR in the liver from the surviving HMGCRKO mice were as high as those from fHMGCR mice (Figure IIB in the online-only Data Supplement). Next, we compared body weight, liver weight, plasma lipid levels, liver functions, and blood glucose levels between fHMGCR and L-HMGCRKO mice (Table). Although the body weight of L-HMGCRKO mice was not different from that of fHMGCR mice at 3 weeks of age, it decreased by 10% at 4 weeks and by 38% at 5 weeks of age. Liver weight did not differ between the 2 groups. However, the ratio of liver weight to body weight was increased by 39% and 74% at 4 and 5 weeks of age, respectively. The livers of L-HMGCRKO mice were enlarged, paler, and whiter than those of fHMGCR mice at 5 weeks of age (Figure 2A and 2B). Consistent with the macroscopic abnormalities of the liver, plasma levels of aspartate aminotransferase, alanine transaminase, and bilirubin were markedly increased in the L-HMGCRKO mice compared with fHMGCR mice at 5 weeks of age. Total cholesterol levels in the plasma were decreased in the L-HMGCRKO mice by 26% at 3 weeks of age (Table). In parallel, plasma concentrations of LDL cholesterol and apolipoprotein (apo) B-100 protein were decreased (Figure IIIA and IIIE in the online-only Data Supplement). Despite the liver failure of L-HMGCRKO mice at 5 weeks of age, the plasma levels of cholesterol, free cholesterol, and phospholipids were increased 4.3-, 7.9-, and 4.0-fold, respectively. On the other hand, plasma cholesterol ester levels were decreased by 38% (Table). Therefore, calculated ratios of free cholesterol to cholesterol ester were increased 13-fold. Most of the increased cholesterol was distributed in the size of very low-density lipoprotein through LDL (Figure IIIC in the online-only Data Supplement). Although apoB-100 levels were decreased, apoB-48 levels were substantially increased in the plasma of L-HMGCRKO mice at 5 weeks of age (Figure IIIG in the online-only Data Supplement). These findings together with the results of agar gel electrophoresis of the plasma (Figure III-I in the online-only Data Supplement) strongly indicate that both lipoprotein X and apoB-48–containing lipoproteins were increased in the L-HMGCRKO mice. Hepatic LDL receptor protein levels were not altered between fHMGCR and L-HMGCRKO mice at 3 and 5 weeks of age (Figure IIIF and IIIH in the online-only Data Supplement), despite increased hepatic LDL receptor mRNA levels (Figure 4A). Plasma lipoprotein changes in L-HMGCRKO mice may not be influenced by LDL receptor protein levels. Plasma free fatty acid levels were also increased 3.1-fold at 5 weeks. In contrast, plasma triglyceride levels were decreased by 69% and 70% at 4 and 5 weeks of age, respectively. It is of note that L-HMRCRKO mice were moderately hypoglycemic at 5 weeks.

To determine the causes of the liver dysfunction associated with hepatomegaly, we performed a microscopic analysis of the liver (Figure 2). Hematoxylin and eosin staining revealed moderate to severe ballooning and unicellular necrosis of parenchymal cells at 5 weeks (Figure 2C and 2D). Oil-red O staining showed moderate to severe microvesicular steatosis of the parenchymal cells (Figure 2E and 2F). TdT-mediated dUTP-nick end labeling–positive (Figure 2G, 2H, and 2M) and Ki-67–positive parenchymal cells

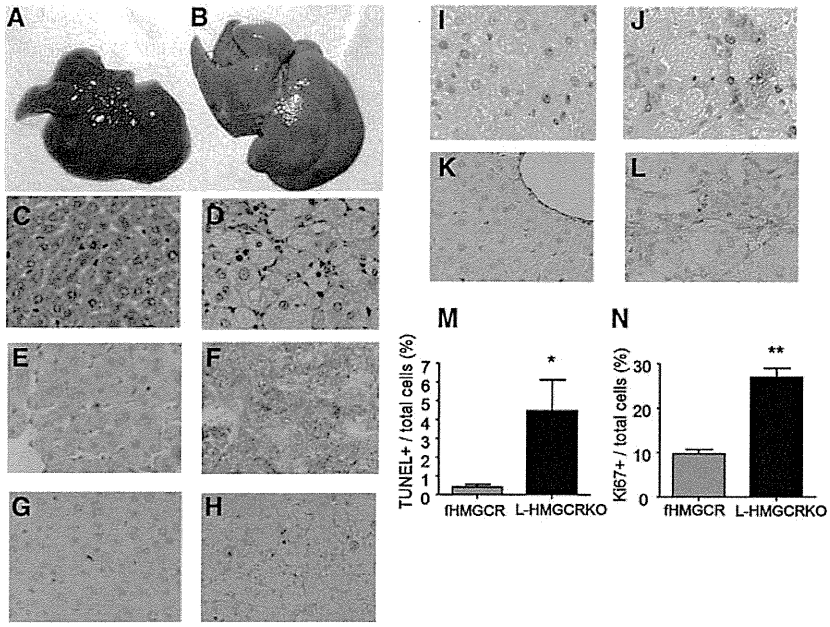

Figure 2. Gross appearance and histological analysis of the livers in male mice at 5 weeks. Gross appearance of the liver from control (**A**) and liver-specific HMGCR knockout (L-HMGCRKO) mice (**B**). Hematoxylin and eosin–stained liver sections from control (**C**) and L-HMGCRKO (**D**) mice. Frozen sections of liver stained with oil-red O from control (**E**) and L-HMGCRKO (**F**) mice. TdT-mediated dUTP-nick end labeling (TUNEL)–stained liver sections from control (**G**) and L-HMGCRKO (**H**) mice. Ki-67–stained liver sections from control (**I**) and L-HMGCRKO (**J**) mice. Type 4 collagen–stained liver sections from control (**K**) and L-HMGCRKO (**L**) mice. Bar graph shows the percentages of TUNEL-positive cells (**M**) and Ki-67–positive cells (**N**) relative to the total number of cells. Each value represents mean±SD. Significant differences compared with control mice: $*P<0.01$ and $**P<0.001$.

(Figure 2I, 2J, and 2N) were significantly increased 11- and 2.8-fold in the liver of L-HMGCRKO mice compared with that in fHMGCR mice, respectively. The liver of L-HMGCRKO mice contained increased amounts of type 4 collagen (Figure 2K and 2L). Caspase 3 activity in the liver of L-HMGCRKO mice was also increased 1.8-fold compared with that of fHMGCR (Figure VA in the online-only Data Supplement). The mRNA levels of C/EBP-homologous protein were also significantly increased (Figure VD in the online-only Data Supplement). However, no significant differences were observed in either caspase 8 activity or H_2O_2 contents in the liver (Figure VB and VC in the online-only Data Supplement). The pathology of the liver from L-HMGCRKO mice at 4 weeks was milder (Figure IVB in the online-only Data Supplement) than that at 5 weeks. The liver of the mice which survived the lethal period still had hepatocyte ballooning (Figure IVD in the online-only Data Supplement).

To determine whether the liver-specific abrogation of HMGCR affected cholesterol metabolism in the liver, we measured the hepatic levels of cholesterol and triglycerides (Figure 3). The hepatic cholesterol content was decreased by only 22% in the L-HMGCRKO mice compared with the fHMGCR mice (Figure 3A). Unexpectedly, the hepatic contents of triglyceride were increased 2-fold (Figure 3B). These results indicate that the neutral lipids stained with oil-red O in the liver were primarily triglycerides. The reduction in the cholesterol contents of the liver was smaller than expected. We measured cholesterol synthesis in liver slices in culture (Figure 3C). The cholesterol synthesis was reduced by 45%. This reduction paralleled the degree of reduction in HMGCR activity in the liver (Figure 1E). We also measured the amounts of fatty acids synthesized in the liver (Figure 3D). Surprisingly, the synthesis of fatty acids from acetate was markedly increased 17-fold in the liver of L-HMGCRKO mice. Although total amounts of fatty acids were not different between the 2 mice (Figure 3E), the following fatty acid species were significantly increased in the liver of L-HMGCRKO mice: C18:0, C18:1n–9, C20:1n–9, C20:3n–9, and C22:4n–6 (Figure 3F). Given the increased production of fatty acids and triglycerides in the liver, we measured other metabolites of fatty acids such as diglycerides and ceramides. The hepatic levels of diglycerides were increased 1.8-fold (Figure 3G), but those of ceramides were not increased significantly (Figure 3H).

To clarify the mechanisms behind the changes in fatty acid metabolism, we determined the changes in the levels of mRNA expression in various genes involved in cholesterol or fatty acid metabolism in the liver at 4 weeks of age by real-time polymerase chain reaction (Figure 4A). As to the genes involved in cholesterol metabolism, the mRNA levels of SREBP2, LDL receptor, proprotein convertase subtilisin/kexin type 9, and squalene synthase were increased 1.4-, 1.9-, 2.8-, and 3.9-fold, respectively. On the other hand, the mRNA levels of cholesterol 7α-hydroxylase, a rate-limiting enzyme for bile acid synthesis, were decreased by 60%. With regard to the genes involved in fatty acid metabolism, the mRNA levels of fatty acid synthase (FAS), acetyl-CoA carboxylase, and stearoyl-CoA desaturase 2 were increased 2.4-, 1.4-, and 22-fold, respectively. On the other hand, the mRNA expression of SREBP1c and acyl CoA:diacylglycerol acyltransferase 2 was decreased by 80% and 40%, respectively. There were no changes in either the mRNA expression of SREBP1a, a splice variant of SREBP1c, or liver X receptor α (LXRα), an important transcriptional activator of the SREBP1c gene. The mRNA expression of peroxisome proliferator–activated receptor α, a transcription regulator of genes for fatty acid oxidation, was not changed.

HMGCR catalyzes the formation of mevalonate, which is used as a substrate for the synthesis not only of cholesterol but also nonsterols such as isoprenoids, ubiquinone, heme A, and dolichol. To test the notion that death, likely because of severe liver failure, was caused by the alteration of a nonsterol pathway, we evaluated the isoprenylation of small GTP-binding proteins such as H-Ras and Rac1 by measuring the amount of membrane-bound forms (Figure 4B). The ratio of the

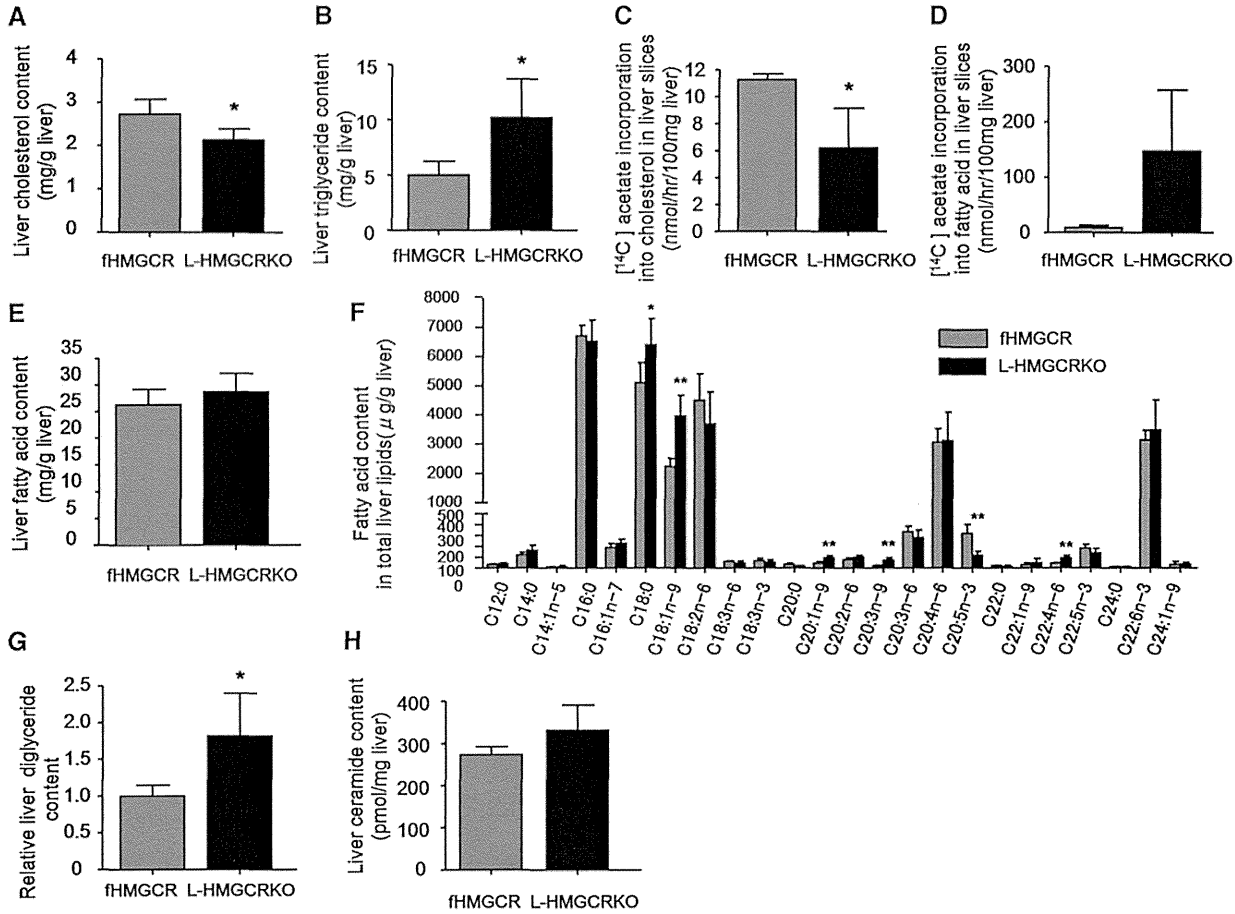

Figure 3. Hepatic lipid contents and lipid synthesis in the control and liver-specific HMGCR knockout (L-HMGCRKO) male mice. Hepatic total cholesterol (**A**), triglyceride (**B**), fatty acid levels (**E**), and fatty acid composition in total liver lipids (**F**) were determined in the livers from control and L-HMGCRKO mice at 4 weeks of age (n=5 in each group). **C** and **D**, In vitro hepatic lipid synthesis rate using the liver slices in culture (n=3 in control and n=4 in L-HMGCRKO). Liver slices (≈100 mg) were incubated with ^{14}C-labeled acetate (8 mmol/L, 0.1 μCi/μmol) for 90 minutes. After incubation, the slices were removed for measurement of ^{14}C-labeled cholesterol (**C**) and fatty acids (**D**). Hepatic diglyceride (**G**) and ceramide (**H**) contents were measured in the livers of control and L-HMGCRKO mice at 4 weeks of age (n=5 in each group) by the diglyceride kinase method as described in the online-only Data Supplement. Each value represents mean±SD. Significant differences compared with control mice: **P*<0.05 and ***P*<0.01.

membrane-bound form to the cytosolic form of H-Ras or Rac1 was decreased to 0.05 to 0.2 compared with control. These results indicate that the deficiency of HMGCR affected the nonsterol pathway more severely than the sterol pathway. We also estimated changes in intracellular signaling molecules (Figure 4C). p-Akt and c-Met were decreased by 72% and 81%, respectively, whereas phospho-signal transducer and activator of transcription 3 was increased 7.6-fold.

If the lethal phenotype of HMGCR deficiency is because of the deficiency of mevalonate, supplementation with mevalonate could theoretically rescue the lethal phenotype. In fact, providing the male mice with water containing mevalonate significantly attenuated the liver dysfunction and hypercholesterolemia (Figure 5A–5C). The pathological abnormalities observed in the male L-HMGCRKO mice were almost normalized by the supplementation with mevalonate (Figure 5D–5G). Consistently, the amounts of the membrane-bound form of H-Ras or Rac 1 were restored to normal levels (Figure 5H). Similar improvements were found in female L-HMGCRKO mice (data not shown). No death occurred until 40 days of age in L-HMGCRKO mice supplemented with mevalonate.

Because L-HMGCRKO mice were hypoglycemic (Table), it is possible that hypoglycemia is the direct cause of death. To test this hypothesis, we allowed mice free access to drinking water containing 20% (w/v) glucose. Glucose feeding significantly increased plasma glucose levels (43.5±16.2 mg/dL [n=10] versus 79.5±40.6 mg/dL [n=13] [*P*=0.01] in males; 36.6±13.3 mg/dL [n=4] versus 65.2±35.6 mg/dL [n=11] [*P*=0.04] in females). Concurrently, it dramatically improved the mortality of L-HMGCRKO mice (96% versus 13% in males and 71% versus 15% in females) (Figure VI in the online-only Data Supplement).

Discussion

Nearly all the male L-HMGCRKO mice died before 40 days of age, whereas 30% of females survived until 12 months of age. Before their death, the mice developed severe hepatic damage with hepatomegaly, steatosis, and hypoglycemia. Thus, we ascribe the lethal effect of the liver-specific deficiency of HMGCR

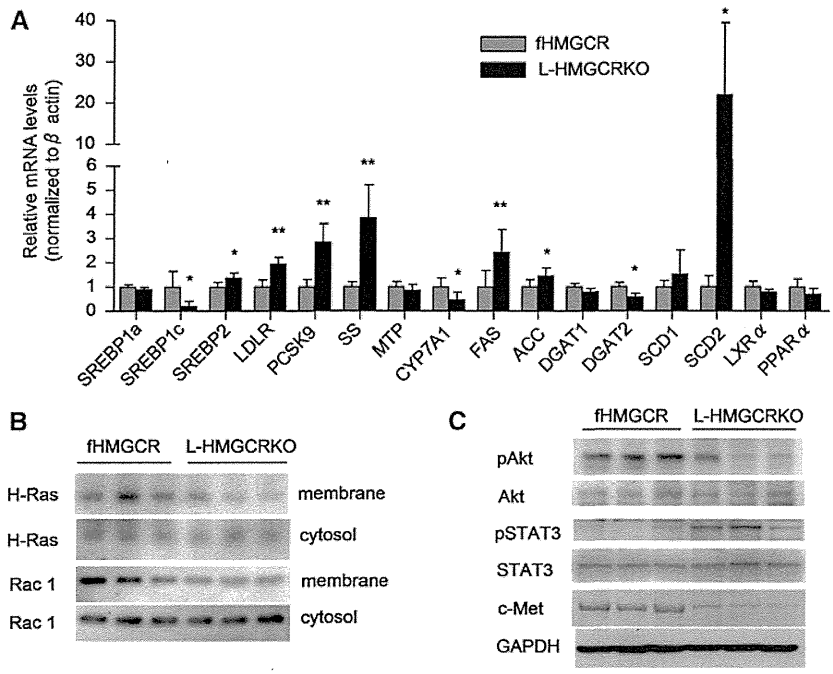

Figure 4. Relative amounts of various mRNAs and degree of isoprenylation of small GTP-binding proteins and liver regeneration-associated proteins in the livers of control and liver-specific HMGCR knockout (L-HMGCRKO) male mice at 4 weeks of age. **A**, Total RNA from the livers of mice (n=5 in each group) was subjected to quantitative real-time polymerase chain reaction as described in the online-only Data Supplement. Each value represents the amount of mRNA relative to that in the control mice, which is arbitrarily defined as 1. **B**, Liver membranous and cytosolic fractions for small GTP-binding proteins or (**C**) liver tissue lysates for liver regeneration-associated proteins were prepared as described in the online-only Data Supplement (n=3 in each group), and aliquots (30 μg) were subjected to SDS-PAGE and immunoblot analysis. Each value represents mean±SD. Significant differences compared with control mice: **P*<0.05 and ***P*<0.01. LDLR indicates low-density lipoprotein receptor; PCSK9, proprotein convertase subtilisin/kexin type 9; FAS, fatty acid synthase; DGAT, diacylglycerol acyltransferase; SCD, stearoyl-CoA desaturase; LXR α, liver X receptor; PPARα, peroxisome proliferator–activated receptor α; SS, squalene synthase; MTP, microsomal triglyceride transfer protein; CYP7A1, cholesterol 7α-hydroxylase; ACC, acetyl-CoA carboxylase; GAPDH, glyceraldehyde-3-phosphate dehydrogenase; STAT3, signal transducer and activator of transcription 3.

to the hepatic toxicity and hypoglycemia. Unexpectedly, the mice developed hypercholesterolemia before death, although hepatic cholesterol synthesis was significantly reduced. This lethal phenotype was completely reversed by mevalonate or glucose, indicating that mevalonate is essential for the survival of mice and that hypoglycemia is the direct cause of lethality.

The mRNA expression of HMGCR was reduced as early as 3 weeks of age and almost undetectable at 4 weeks. This developmental reduction in the expression is consistent with the developmental induction of the expression of albumin. Other liver-specific KO models using Alb-Cre showed abrogation of the expression of reporter genes at a similar stage.[12] However, the HMGCR activity of the liver was reduced by only 50%. Because the parenchymal hepatocytes from the liver of the L-HMGCRKO mice at 3 weeks of age expressed substantial HMGCR activity, we speculate that most of the activity is derived from upregulated HMGCR expression in a certain subset of hepatocytes that escaped from HMGCR gene inactivation. Indeed, recombination efficiency was only 75% at weaning,[13] and HMGCR protein can be increased 25-fold at the posttranscriptional level.[1]

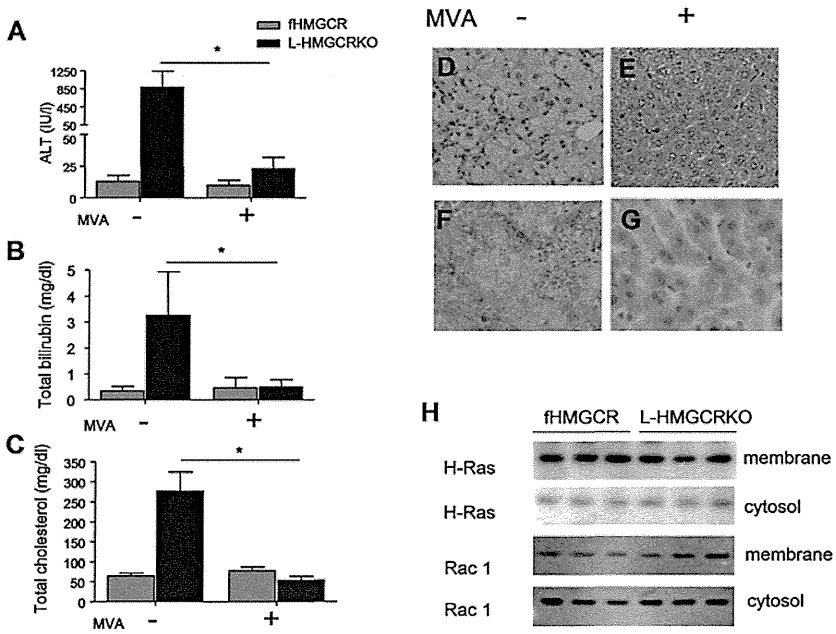

Figure 5. Supplementation of mevalonate. Male mice were given mevalonate in drinking water at a concentration of 5 mmol/L from the age of 28 days to 35 days (n=5 in each group). After supplementation, plasma alanaine transaminase (ALT) (**A**), total bilirubin (**B**), and total cholesterol (**C**) levels were measured. The livers were removed from liver-specific HMGCR knockout (L-HMGCRKO) mice not supplemented with mevalonate (–; **D** and **F**, respectively) or supplemented with mevalonate (+; **E** and **G**, respectively) stained with hematoxylin and eosin or oil-red O. **H**, Immunoblot analyses for small GTP-binding proteins in membranous and cytosolic fractions of the liver. Each value represents mean±SD. Significant differences compared with control mice: **P*<0.001.

Furthermore, there might be time lag between disappearance of HMGCR protein and cessation of transcription.

Sex dimorphism in lethality is noteworthy. The present results that male L-HMGCRKO mice were more prone to die than females are consistent with the general view that females are more resistant to morbidity and mortality of various liver diseases than males.[14] In addition to protection against liver injury via vasodilating and anti-inflammatory effects, estrogen itself attenuates the development of hepatic steatosis.[15] The mRNA expression levels of HMGCR in the liver of the surviving L-HMGCRKO mice were indistinguishable from those of fHMGCR mice (Figure IIB in the online-only Data Supplement). It is likely that the hepatocytes with a relatively intact HMGCR gene may be extensively regenerated, thereby eventually compensating for the KO in the survivors. In support of this, several Ki-67–positive cells were greatly increased in the L-HMGCRKO mice (Figure 2L and 2N).

Hepatic cholesterol levels were mildly decreased, and the decrease in plasma cholesterol levels was modest in the L-HMGCRKO mice at 3 weeks of age. More surprisingly, the plasma cholesterol levels even increased immediately before death. Extrahepatic organs with high cholesterol synthesis, such as skin, bowels, and muscles, may be a source of cholesterol in the plasma.[16] The hypercholesterolemia before death appears paradoxical, given the failure of cholesterol synthesis in the hepatocytes. At this stage, the mice develop jaundice. Because the physicochemical characteristics of the accumulated lipoproteins were similar to those of lipoprotein X, cholestasis may at least partly account for hypercholesterolemia. Simultaneous accumulation of both lipoprotein X and apoB48-containing particles has also been reported in rats with intrahepatic cholestasis.[17]

Interestingly, L-HMGCRKO mice showed hepatic steatosis. Because hepatic triglyceride levels were increased 2-fold but hepatic cholesterol ester levels were not increased (data not shown) most of the neutral lipids stained with oil-red O are triglycerides. Supporting this, the synthesis of fatty acids was increased 17-fold. In this context, it is noteworthy that the expression of enzymes for fatty acid synthesis, FAS and stearoyl-CoA desaturase 2, was increased. In normal adults, stearoyl-CoA desaturase 1 is the major enzyme catalyzing desaturation of oleate, whereas stearoyl-CoA desaturase 2 is an isozyme that is transiently expressed in the liver in embryos and neonates and may be involved in lipogenesis at that developmental stage.[18] Indeed, the amounts of polyunsaturated fatty acids were increased in the liver (Figure 3F).

The increase in fatty acids synthesis appeared disproportionately larger than the increase in triglycerides in the liver. In this context, it is of note that the expression of diacylglycerol acyltransferase 1 was not increased and that of diacylglycerol acyltransferase 2 was even decreased. Thus, it is probable that the newly synthesized fatty acids were not used to produce triglycerides. Generally, the enzymes catalyzing fatty acid synthesis are transcriptionally induced by SREBP1c. However, the expression of SREBP1c was reduced 5-fold, suggesting that the increased lipogenesis was not mediated by SREBP1c. Similar SREBP1c-independent lipogenesis is reported in mice overexpressing a constitutively active form of Akt in the liver.[19] Furthermore, the levels of LXRα mRNA, a nuclear receptor that can stimulate SREBP1c gene expression[20] and can also directly stimulate transcription of FAS,[21] were not increased in the livers of L-HMGCRKO mice. We speculate that the lack of cholesterol reduces the supply of oxysterols, physiological ligands of LXR, which transactivates SREBP1c.[22] This notion is supported by the decreased expression of cholesterol 7α-hydroxylase and diacylglycerol acyltransferase 2, also targets of LXR.

In contrast to SREBP1c expression, the expression of SREBP2 was increased, conceivably accounting for the increased expression of its targets: the LDL receptor and squalene synthase. The expression of FAS in the face of significant suppression of SREBP1c or unaltered LXRα suggests a regulatory pathway independent of SREBP1c or LXRα. Recently, a decrease in farnesyl pyrophosphate or farnesol has been shown to induce the expression of FAS independently of SREBP1c.[23]

The liver of the L-HMGCRKO mice contained increased numbers of TdT-mediated dUTP-nick end labeling–positive cells. Consistent with the apoptotic nature of the cell death, the activity of caspase 3, a final executer of apoptosis which cleaves to induce the release of cytochrome c from mitochondria, was increased in the liver of the L-HMGCRKO mice. We have hypothesized several potential mechanisms for apoptosis: accumulation of toxic lipid metabolites[24] and reduction of survival factors.[25] However, we failed to obtain evidence for the involvement of ceramide and survivin in apoptosis.

As predicted, membrane-bound forms of Ras and Rac1 were significantly reduced, conceivably as a result of the defect in their isoprenylation. Several mechanisms linking the defect in isoprenylation to apoptosis have been proposed. For example, Rac1 is reported to protect against apoptosis by stimulating nicotinamide adenine dinucleotide phosphate-oxidase, thereby increasing the levels of reactive oxygen species.[26] However, we failed to detect a decrease in H_2O_2 levels in the liver.

During the search for the plausible mechanism of the hepatocyte apoptosis, we found a significant increase in the mRNA level of C/EBP-homologous protein, a hallmark of the ER stress response and inducer of apoptosis, in the liver of L-HMHCRKO mice. Because hepatic steatosis induces ER stress, it is reasonable to speculate that the increased synthesis of fatty acids causes hepatic lipoapoptosis via increasing the C/EBP-homologous protein. The liver of L-HMGCRKO mice had significantly decreased levels of either p-Akt or c-met protein. Because hepatocyte growth factor exerts prosurvival effects mainly through activating phosphatidylinositol-3 kinase/Akt pathway after binding to its receptor, c-met,[27] defective hepatocyte growth factor signaling may play a salutary role in the induction of hepatocyte apoptosis. The increase in phospho-signal transducer and activator of transcription 3 might be a compensatory response secondary to increased apoptosis, but failed to overcome it. Similar failure to compensate the liver failure by activated signal transducer and activator of transcription 3 was reported in mice deficient in phosphoinositide-dependent protein kinase 1.[28]

These phenotypes of L-HMGCRKO mice should be discussed in relation to other mouse models of genetic disorders of cholesterol metabolism. Thus far, 2 models have been reported to survive the perinatal period, despite reduced cholesterol biosynthesis in the liver. Because the global disruption of SREBP cleavage-activating protein and site 1 protease is embryonic lethal, as is the case for HMGCR, liver-specific KO

mice have been generated. In both the liver-specific SREBP cleavage-activating protein[29] and site 1 protease KO mice,[30] the synthesis of cholesterol as well as fatty acids was significantly reduced in the liver. Neither mouse, however, died of liver toxicity, probably because the reduction in the expression of HMGCR was not as severe as in L-HMGCRKO mice.

In conclusion, HMGCR is essential for the survival of mice. Despite the defect in hepatic cholesterol biosynthesis in L-HMGCRKO mice, the homeostasis of cholesterol in the liver and plasma is surprisingly well maintained presumably via compensatory changes in the flux of cholesterol and fatty acids. These results might provide insight for understanding the role of cholesterol biosynthetic pathway in the normal function of hepatocytes.

Acknowledgments

We thank Drs Derek LeRoith, Wataru Ogawa, and Masato Kasuga for providing Alb-Cre mice. We also thank Drs Tetsuya Kitamine, Ryuichi Tozawa, Yoshiaki Tamura, Hiroaki Okazaki, Masaki Igarashi, Hitoshi Shimano, and Nobuhiro Yamada for their help and discussion.

Sources of Funding

This work was supported by a Grant-in-Aid for Scientific Research from the Ministry of Education, Science and Culture and the Program for Promotion of Fundamental Studies in Health Sciences of the National Institute of Biomedical Innovation (NIBIO) and JKA through its promotion funds from KEIRIN RACE.

Disclosures

None.

References

1. Goldstein JL, Brown MS. Regulation of the mevalonate pathway. *Nature*. 1990;343:425–430.
2. Liscum L, Finer-Moore J, Stroud RM, Luskey KL, Brown MS, Goldstein JL. Domain structure of 3-hydroxy-3-methylglutaryl coenzyme A reductase, a glycoprotein of the endoplasmic reticulum. *J Biol Chem*. 1985;260:522–530.
3. Hua X, Nohturfft A, Goldstein JL, Brown MS. Sterol resistance in CHO cells traced to point mutation in SREBP cleavage-activating protein. *Cell*. 1996;87:415–426.
4. Sever N, Yang T, Brown MS, Goldstein JL, DeBose-Boyd RA. Accelerated degradation of HMG CoA reductase mediated by binding of insig-1 to its sterol-sensing domain. *Mol Cell*. 2003;11:25–33.
5. Kathiresan S, Melander O, Guiducci C, Surti A, Burtt NP, Rieder MJ, Cooper GM, Roos C, Voight BF, Havulinna AS, Wahlstrand B, Hedner T, Corella D, Tai ES, Ordovas JM, Berglund G, Vartiainen E, Jousilahti P, Hedblad B, Taskinen MR, Newton-Cheh C, Salomaa V, Peltonen L, Groop L, Altshuler DM, Orho-Melander M. Six new loci associated with blood low-density lipoprotein cholesterol, high-density lipoprotein cholesterol or triglycerides in humans. *Nat Genet*. 2008;40:189–197.
6. Endo A, Kuroda M, Tanzawa K. Competitive inhibition of 3-hydroxy-3-methylglutaryl coenzyme A reductase by ML-236A and ML-236B fungal metabolites, having hypocholesterolemic activity. *FEBS Lett*. 1976;72:323–326.
7. Baigent C, Keech A, Kearney PM, Blackwell L, Buck G, Pollicino C, Kirby A, Sourjina T, Peto R, Collins R, Simes R; Cholesterol Treatment Trialists' (CTT) Collaborators. Efficacy and safety of cholesterol-lowering treatment: prospective meta-analysis of data from 90,056 participants in 14 randomised trials of statins. *Lancet*. 2005;366:1267–1278.
8. Liao JK, Laufs U. Pleiotropic effects of statins. *Annu Rev Pharmacol Toxicol*. 2005;45:89–118.
9. Ohashi K, Osuga J, Tozawa R, Kitamine T, Yagyu H, Sekiya M, Tomita S, Okazaki H, Tamura Y, Yahagi N, Iizuka Y, Harada K, Gotoda T, Shimano H, Yamada N, Ishibashi S. Early embryonic lethality caused by targeted disruption of the 3-hydroxy-3-methylglutaryl-CoA reductase gene. *J Biol Chem*. 2003;278:42936–42941.
10. Tozawa R, Ishibashi S, Osuga J, Yagyu H, Oka T, Chen Z, Ohashi K, Perrey S, Shionoiri F, Yahagi N, Harada K, Gotoda T, Yazaki Y, Yamada N. Embryonic lethality and defective neural tube closure in mice lacking squalene synthase. *J Biol Chem*. 1999;274:30843–30848.
11. Yakar S, Liu JL, Stannard B, Butler A, Accili D, Sauer B, LeRoith D. Normal growth and development in the absence of hepatic insulin-like growth factor I. *Proc Natl Acad Sci USA*. 1999;96:7324–7329.
12. Inoue H, Ogawa W, Ozaki M, Haga S, Matsumoto M, Furukawa K, Hashimoto N, Kido Y, Mori T, Sakaue H, Teshigawara K, Jin S, Iguchi H, Hiramatsu R, LeRoith D, Takeda K, Akira S, Kasuga M. Role of STAT-3 in regulation of hepatic gluconeogenic genes and carbohydrate metabolism in vivo. *Nat Med*. 2004;10:168–174.
13. Postic C, Magnuson MA. DNA excision in liver by an albumin-Cre transgene occurs progressively with age. *Genesis*. 2000;26:149–150.
14. Yokoyama Y, Nimura Y, Nagino M, Bland KI, Chaudry IH. Current understanding of gender dimorphism in hepatic pathophysiology. *J Surg Res*. 2005;128:147–156.
15. Nemoto Y, Toda K, Ono M, Fujikawa-Adachi K, Saibara T, Onishi S, Enzan H, Okada T, Shizuta Y. Altered expression of fatty acid-metabolizing enzymes in aromatase-deficient mice. *J Clin Invest*. 2000;105:1819–1825.
16. Spady DK, Dietschy JM. Sterol synthesis in vivo in 18 tissues of the squirrel monkey, guinea pig, rabbit, hamster, and rat. *J Lipid Res*. 1983;24:303–315.
17. Chisholm JW, Dolphin PJ. Abnormal lipoproteins in the ANIT-treated rat: a transient and reversible animal model of intrahepatic cholestasis. *J Lipid Res*. 1996;37:1086–1098.
18. Miyazaki M, Dobrzyn A, Elias PM, Ntambi JM. Stearoyl-CoA desaturase-2 gene expression is required for lipid synthesis during early skin and liver development. *Proc Natl Acad Sci USA*. 2005;102:12501–12506.
19. Ono H, Shimano H, Katagiri H, Yahagi N, Sakoda H, Onishi Y, Anai M, Ogihara T, Fujishiro M, Viana AY, Fukushima Y, Abe M, Shojima N, Kikuchi M, Yamada N, Oka Y, Asano T. Hepatic Akt activation induces marked hypoglycemia, hepatomegaly, and hypertriglyceridemia with sterol regulatory element binding protein involvement. *Diabetes*. 2003;52:2905–2913.
20. Chen G, Liang G, Ou J, Goldstein JL, Brown MS. Central role for liver X receptor in insulin-mediated activation of Srebp-1c transcription and stimulation of fatty acid synthesis in liver. *Proc Natl Acad Sci USA*. 2004;101:11245–11250.
21. Joseph SB, Laffitte BA, Patel PH, Watson MA, Matsukuma KE, Walczak R, Collins JL, Osborne TF, Tontonoz P. Direct and indirect mechanisms for regulation of fatty acid synthase gene expression by liver X receptors. *J Biol Chem*. 2002;277:11019–11025.
22. Yoshikawa T, Shimano H, Amemiya-Kudo M, Yahagi N, Hasty AH, Matsuzaka T, Okazaki H, Tamura Y, Iizuka Y, Ohashi K, Osuga J, Harada K, Gotoda T, Kimura S, Ishibashi S, Yamada N. Identification of liver X receptor-retinoid X receptor as an activator of the sterol regulatory element-binding protein 1c gene promoter. *Mol Cell Biol*. 2001;21:2991–3000.
23. Murthy S, Tong H, Hohl RJ. Regulation of fatty acid synthesis by farnesyl pyrophosphate. *J Biol Chem*. 2005;280:41793–41804.
24. Anderson N, Borlak J. Molecular mechanisms and therapeutic targets in steatosis and steatohepatitis. *Pharmacol Rev*. 2008;60:311–357.
25. Kaneko R, Tsuji N, Asanuma K, Tanabe H, Kobayashi D, Watanabe N. Survivin down-regulation plays a crucial role in 3-hydroxy-3-methylglutaryl coenzyme A reductase inhibitor-induced apoptosis in cancer. *J Biol Chem*. 2007;282:19273–19281.
26. Deshpande SS, Angkeow P, Huang J, Ozaki M, Irani K. Rac1 inhibits TNF-alpha-induced endothelial cell apoptosis: dual regulation by reactive oxygen species. *FASEB J*. 2000;14:1705–1714.
27. Xiao GH, Jeffers M, Bellacosa A, Mitsuuchi Y, Vande Woude GF, Testa JR. Anti-apoptotic signaling by hepatocyte growth factor/Met via the phosphatidylinositol 3-kinase/Akt and mitogen-activated protein kinase pathways. *Proc Natl Acad Sci USA*. 2001;98:247–252.
28. Haga S, Ozaki M, Inoue H, Okamoto Y, Ogawa W, Takeda K, Akira S, Todo S. The survival pathways phosphatidylinositol-3 kinase (PI3-K)/phosphoinositide-dependent protein kinase 1 (PDK1)/Akt modulate liver regeneration through hepatocyte size rather than proliferation. *Hepatology*. 2009;49:204–214.
29. Matsuda M, Korn BS, Hammer RE, Moon YA, Komuro R, Horton JD, Goldstein JL, Brown MS, Shimomura I. SREBP cleavage-activating protein (SCAP) is required for increased lipid synthesis in liver induced by cholesterol deprivation and insulin elevation. *Genes Dev*. 2001;15:1206–1216.
30. Yang J, Goldstein JL, Hammer RE, Moon YA, Brown MS, Horton JD. Decreased lipid synthesis in livers of mice with disrupted Site-1 protease gene. *Proc Natl Acad Sci USA*. 2001;98:13607–13612.

Supplemental material

Supplemental Methods

Generation of mice heterozygous for the floxed HMGCR allele

A conditional targeting vector of a replacement type was produced by inserting a loxP site into a XhoI site in intron 1 and loxP-flanked (floxed) polII-neo-bpA cassette into a BamHI site in intron 4 (Supplemental figure I). The transcriptional orientation of the neo gene was opposite to that of the HMGCR gene. Excision of sequences between the loxP sites by Cre recombinase deletes exons 2 to 4, which includes the initiator methionine and residues encoding the first membrane-bound domain of HMHCR. JH1 ES cells (A gift from Dr. J. Herz) were electroporated with the targeting vector as described[1]. Recombinant clones containing a single floxed HMGCR allele were identified by PCR using primers primers P1 (5'-ACGAAAGGGCCTCGTGATACGCCTA-3') and P2 (5'-ATGTCTGCAGTCCCAGCACTCAGCT-3'). All targeted clones were confirmed by Southern blot analysis using a cDNA probe containing exons 7-10. The targeted clones were injected into the C57BL/6J blastocysts, yielding two lines of chimeric mice which transmitted the floxed allele through the germ line.

Generation of liver specific HMGCR knockout mice.